European Journal of Histochemistry 2025; volume 69:4239

miR-199a-5p inhibited HIF-1α to suppress the proliferation, migration, and differentiation of cardiac stem cells

Sha Li,[1] Cuigai Zhang,[1] Yanping Liu,[1] Cuiqiao Meng,[1] Yang Xie,[1] Shuren Li[2]1

[1]Medical Examination Center; [2]Department of Cardiovascular Diseases, Hebei General Hospital, Shijiazhuang City, Hebei, China

ABSTRACT

The cardiac stem cells (CSCs) are essential in improving myocardial infarction (MI). Although miR-199a-5p and hypoxia-inducible factor-1 alpha (HIF-1α) were proven to participate in the process of heart repair, the related mechanisms are still unclear. This study aimed to explore the effects of miR-199a-5p and HIF-1α on c-kit$^+$ cells and their regulatory mechanisms. After isolating, purifying, and identifying CSCs (c-kit$^+$ cells) from mice, they were subjected to a hypoxia model. After the c-kit$^+$ cells were transfected with corresponding transfectants, the CCK-8, EdU staining, and wound healing approaches were used to evaluate their cell viability, proliferation, and migration. The targeted relation between miR-199a-5p and HIF-1α was determined using a dual-luciferase reporter. Immunofluorescence staining, RT-qPCR, and Western blot approaches were employed to determine Nkx2.5, CD31, α-SMA, miR-199a-5p, and HIF-1α expression. Overexpressing miR-199a-5p and knocking down HIF-1α both inhibited the cell viability ($p<0.01$), reduced the proliferation ($p<0.05$), suppressed the migration ($p<0.001$), and downregulated the Nkx2.5, CD31, and α-SMA expression of c-kit$^+$ cells ($p<0.05$). Overexpressing HIF-1α effectively reversed the effects of overexpressing miR-199a-5p on c-kit$^+$ cells ($p<0.05$). Taken together, miR-199a-5p negatively targeted HIF-1α to inhibit the proliferation, migration, and differentiation of c-kit$^+$ cells.

Key words: c-kit$^+$ cardiac stem cells; miR-199a-5p; HIF-1α.

Correspondence: Shuren Li, Department of Cardiovascular Diseases, Hebei General Hospital, No. 348 Heping West Road, Shijiazhuang City, Hebei Province, China. E-mail: 17778268087@163.com

Contributions: all authors made a substantive intellectual contribution, read and approved the final version of the manuscript and agreed to be accountable for all aspects of the work.

Conflict of interest: the authors declare no competing interests, and all authors confirm accuracy.

Ethics approval: this study was approved by the Animal Ethics Committee of Hebei General Hospital Animal Center (Approval no. HG-23-EC-107). The experiments were approved by the Animal Care and Utilization Committee of Hebei General Hospital and the protocols complied with the guidelines for the welfare and use of animals in cancer research.

Availability of data and materials: the dataset generated or analyzed in this study are available from the corresponding author on reasonable request.

Funding: this research did not receive any specific grant from funding agencies in the public, commercial, or not-for-profit sectors.

Introduction

Myocardial infarction (MI) severely threatens human health, which induces the reduction of the number of cardiomyocytes and even cardiomyocyte necrosis. Due to the lack of regenerative ability in mature cardiomyocytes, the infarcted myocardium is replaced by non-contractile scar tissue through fibrosis to maintain cardiac function, which induces ventricular remodeling.[1] The ventricular remodeling, characterized by disorder of myocardial structure, decreased contractility, insufficient blood supply, and impaired myocardial contraction and relaxation function, ultimately progresses to heart failure and sudden death.[2] The current therapies have made great progress in treating MI, such as the early intervention therapy that opens occluded blood vessels, the coronary artery bypass graft that restores blood supply in the distal occluded blood vessels, and drug treatments that improve symptoms and reduce the risk of coronary heart disease. However, these methods cannot meet the requirements to prevent apoptosis after the blood reconstruction. In addition, although heart transplantation fundamentally achieves the therapeutic goal, the immune exclusion reactions, limited donor numbers, and high costs limit its clinical application.[3] Therefore, stem cells with biological functions of replacing, repairing, and enhancing damaged myocardial tissue have become a research hotspot for MI treatment.

Although cardiac stem cells (CSCs) contribute to treating MI because they can differentiate into cardiac cell lines, the specific mechanisms of CSCs for the treatment of MI are still not entirely clear.[4] There are currently two main perspectives for CSCs in treating MI, namely the direct differentiation effect and the paracrine effects. Many studies have shown that the isolated CSCs directly differentiate into diverse cell types related to the cardiovascular system *in vitro*, and promote the improvement of cardiac function after being transplanted into ischemic areas *in vivo*.[5,6] In addition, an increasing number of studies indicated that transplanted CSCs exert their therapeutic effects on cardiovascular diseases by secreting cytokines or growth factors, namely hypoxia-inducible factor-1 alpha (HIF-1α).[7] Previous studies demonstrated that HIF-1α facilitated the migration, proliferation, differentiation, and angiogenesis of CSCs *in vitro* and recruited endogenous CSCs to inhibit apoptosis of infarcted cardiomyocytes, resist myocardial remodeling, and improve cardiac function *in vivo*.[8,9] However, it is not yet clear which factor regulates HIF-1α expression after MI. Therefore, we aim to investigate the upstream regulatory mechanisms of HIF-1α in CSCs, providing novel therapeutic targets for MI.

With the increasing studies on ncRNAs (including miRNAs, lncRNAs, circRNAs), it gradually recognized that ncRNAs have made great contribution in treating cardiovascular diseases, especially for MI.[10-12] MiRNAs, with a length of approximately 22 nucleotides, contribute to treating pathological cardiac hypertrophy, MI, and arrhythmia by regulating the effects after CSCs transplantation, such as differentiating into cardiomyocytes and paracrine effects.[13] miR-199a-5p, one of miRNAs, participates in multiple cardiovascular diseases because of its essential role in modulating stem cell differentiation, angiogenesis, and apoptosis.[14] It was demonstrated that miR-199a-5p promotes osteogenic differentiation of human stem cells.[15] However, the roles of miR-199-5p in CSCs are still unclear. It was reported that overexpressing miR-199a-5p inhibited the angiogenesis of human renal microvascular endothelial cells and promoted cell apoptosis by regulating Wnt7b/Wnt/β-catenin signaling pathway.[16] It was also affirmed that the intravenous delivery of miR-199a-5p into rats contributed to the repair of MI, and the miR-199a-5p-mediated SIRT1/P300/Yy1/sST2 signaling pathway participated in regulating MI.[17,18] It can be seen that the investigation and intervention targeting miR-199a-5p are expected to be novel strategies for preventing and treating MI. However, it is still unclear whether miR-199a-5p alleviates MI by regulating HIF-1α. Therefore, after isolating, purifying, and identifying c-kit$^+$ cells (one kind of CSCs) from mice, they were subjected to a hypoxia model, one extensively used *in vitro* model to simulate MI. Meanwhile, the c-kit+ cells were respectively transfected with miR-199a-5p mimics, si-HIF-1α, and oe-HIF-1α to investigate the effects of miR-199a-5p and HIF-1α on c-kit$^+$ cells and their related regulatory mechanisms, providing a novel therapeutic strategy for MI.

Materials and Methods

Materials

IMEM culture medium (Lot. A1048901), DMEM/F12 culture medium (Lot. 12634010), fetal bovine serum (FBS, Lot. A5670701), and 0.1% collagenase II (Lot. 17101015) were purchased from Gibco (Grand Island, NY, USA). Lipofectamine TM 3000 (Lot. L3000015) was bought from Thermo Fisher Scientific (Waltham, MA, USA). The CCK-8 agent (Lot. BA00208) was obtained from Bioss (Beijing, China). The EdU staining kit (Lot. C0071S), the dual-luciferase reporter gene detection kit (Lot. RG027), and the Trizol agent (Lot. R0016) were bought from Beyotime (Shanghai, China). The HiScript lll 1st strand cDNA synthesis kit (Lot. R312) and Taq pro universal SYBR qPCR master mix (Lot. Q712) were bought from Vazyme (Nanjing, China). The antibodies of c-kit (Lot. ab317843), CD34 (Lot. ab316277), CD45 (Lot. ab317446), Nkx2.5 (Lot. ab97355), CD31 (Lot. ab222783), and α-SMA (Lot. ab7817) were purchased from Abcam (Cambridge, UK). The antibodies of HIF-1α (Lot. 82989-4-PBS), β-Tubulin (Lot. #2146), and Scal-1 (Lot. 12-5981-82) were bought from Proteintech (Wuhan, China), Cell Signaling Technology (Danvers, MA, USA), and ThermoFisher Scientific, respectively.

Isolation and culture of CSCs

The CSCs were isolated according to the previous study.[19] All two-month-old male C57BL/6 mice (weighing 18-23 g) were adaptively fed in Guangzhou Laidi Biomedical Research Institute Co., Ltd for two weeks. During the adaptive periods, the mice had free access to food and water in surroundings of about 22°C and approximately 55% humidity. After finishing the adaptation and being anesthetized with pentobarbital sodium, mice were executed. The hearts were isolated and cut into tissue blocks (1 × 1 × 1 cm) on the sterile workbench. After that, the tissue blocks were transferred into the digestive enzyme that was composed of 0.25% trypsin and 0.1% collagenase II at 37°C. Then, the digested myocardial tissue was incubated with a Matrigel-covered cell culture plate for 2 weeks at 37°C. Finally, the survived cells on the plate were digested by the Accutase™ enzyme and transferred into a medium composed of 78% IMDM culture medium supplemented with β-mercaptoethanol, 20% FBS, and 1% L-glutamine, penicillin, and streptomycin for further culture.

Purification and culture of c-kit$^+$ cells

The c-kit$^+$ cells were purified based on the immunomagnetic bead separation approach.[20] After the cells were collected, they were washed by 500 μL buffer twice and incubated with 10 μL c-kit-labeled beads at 4°C for 15 min. Then, after supplementing with 500 μL buffer, the mixed solution was loaded into a separation column. The effluent was gathered and transferred to a cell

culture dish supplemented with the cultural medium composed of 86% DMEM/F12 culture medium supplemented with β-mercaptoethanol, 10% FBS, 2% B27 serum-free additive, 1% L-glutamine, 1% penicillin, and streptomycin for further culture.

Identification of c-kit$^+$ cells

After collecting the effluent cells, they were resuspended and respectively incubated with FITC-c-kit antibody, FITC-Sca-1 antibody, FITC-CD34 antibody, and FITC-CD45 antibody at 4°C for 30 min in the dark. After that, the c-kit, Sca-1, CD34, and CD45 expression of approximately 1×10^4 cells was determined by three independent experiments using an Attune NxT flow cytometer (Thermo Fisher Scientific) after additionally supplementing with 400 μL buffer.

Cell transfection

The employed lentivirus transfectants in the present study, including NC mimics, miR-199a-5p mimics, si-NC, si-HIF-1α, oe-NC, and oe-HIF-1α, were synthesized and bought from Sangon Biotech (Shanghai, China). After identifying c-kit$^+$ cells, the corresponding lentivirus transfectants were co-cultured with them for 72 h to accomplish the transfection following the operation instructions of Lipofectamine TM 3000.

Hypoxia model

The hypoxia model was performed according to the previous study with a slight modification.[21] In brief, the logarithmically growing c-kit$^+$ cells were transferred into an anoxic surrounding (1% O_2, 5% CO_2, and 94% N_2) for a 24 h to accomplish the hypoxia model.

Cell experiment protocol

To investigate the effects of miR-199a-5p on c-kit$^+$ cells, they were randomly separated into three groups, namely the control, NC mimics, and miR-199a-5p mimics groups. Apart from c-kit$^+$ cells in the control group being conventionally cultured, cells in the other two groups were transfected with the corresponding transfectants. To investigate the effects of inhibiting HIF-1α on c-kit$^+$ cells under the hypoxic environment, they were stochastically separated into four groups, namely the control, model, si-NC, and si-HIF-1α groups. Apart from the c-kit$^+$ cells in the control group being conventionally cultured, the c-kit$^+$ cells in other groups were exposed to the hypoxia condition. Besides, the c-kit$^+$ cells in the last two groups were transfected with the corresponding transfectants. To investigate whether overexpressing HIF-1α reversed the effects of miR-199a-5p on c-kit$^+$ cells under hypoxic surroundings, they were randomly separated into six groups, including the control, model, NC mimics, miR-199a-5p mimics, miR-199a-5p mimics + oe-NC, and miR-199a-5p mimics + oe-HIF-1α groups. The c-kit$^+$ cells in the control group were conventionally cultured and were exposed to the hypoxia condition in the other groups. Cells in the last four groups were transfected with the corresponding transfectants.

CCK-8

In short, after finishing the corresponding operations, the 10 μL CCK-8 was incubated with c-kit$^+$ cells. Then, the absorbance at 450 nm was measured, and cell viability was calculated based on absorbance.

EdU staining

Generally, after accomplishing the corresponding operations, the EdU solution was incubated with c-kit$^+$ cells. After that, cells were further immersed in the Click-iT mixture in the dark after they were fixed with 4% paraformaldehyde. Finally, cells were immersed in DAPI for 5 min in the dark at room temperature before they were visualized in three different fields under a magnification of 200× using a BZ-H4XD fluorescence microscope (Keyence, Osaka, Japan). With the help of Image J, the positively stained rate of EdU was determined to assay cell proliferation in three independent experiments.

Wound healing assay

In short, after completing the corresponding operations, the vertical parallel scratches with a space of 1 cm were conducted. Then, c-kit$^+$ cells were incubated in the serum-free medium for a further 24 h. The widths of scratches of c-kit$^+$ cells at 0 h and 24 h were quantified using ImageJ to assay migration.

Immunofluorescence

In brief, after finishing the corresponding operations, c-kit$^+$ cells cultured on the cell crawling slide were fixed with 4% paraformaldehyde for 15 min. For the determination of Nkx2.5, after c-kit$^+$ cells were permeabilized by 0.5% TritonX-100 for 5 min and blocked by the bovine serum albumin for 40 min at room temperature, they were incubated with anti-Nkx2.5 (1:2000) overnight at 4°C and immersed in the Cy3-labeled goat anti-rabbit antibody (1:200) for 50 min. Finally, after being stained by DAPI, c-kit$^+$ cells were visualized in three different fields under a magnification of 200× using the fluorescence microscope. The difference in the procedure between determining α-SMA and determining Nkx2.5 was that the 0.5% TritonX-100 was not used. The differences in the procedure between determining CD31 and determining Nkx2.5 were that the 0.5% TritonX-100 was not used, and the FITC-labeled goat anti-rabbit antibody (1:200) was used as the secondary antibody. The immunofluorescence staining was performed in three independent experiments, and the stained results without incubating with primary antibodies were considered as the negative control. The ImageJ software was used to evaluate the fluorescence intensity of positively stained Nkx2.5 co-located with the nucleus and positively stained α-SMA and CD31 around the nucleus.

Dual-luciferase report

The potential targeted relation between miR-119a-5p and HIF-1α was predicted by the Target Scan website (http://targetscan.org/). After the wild-type and mutant-type 3'UTR of HIF-1α were respectively cloned into luciferase vectors, the luciferase activity of c-kit$^+$ cells that were respectively transfected with the above vectors, NC mimics, and miR-119a-5p mimics was detected.

RT-qPCR

After the total RNAs in c-kit$^+$ cells with corresponding operations were extracted by using the Trizol agent, the cDNAs were synthesized by reverse transcription of RNAs. Then, the cDNA amplification was performed. The reverse transcription and amplification processes were performed in the RT-qPCR instrument. Gene expression levels were calculated using the $2^{-\Delta\Delta Ct}$ approach. The sequences of upstream and downstream primers are listed in Table 1, among which U6 and GAPDH are internal references.

Western blot

After proteins in c-kit$^+$ cells with corresponding operations were isolated by RIPA lysis solution, the total proteins were denatured in boiling water. Then, the denatured proteins were loaded on an SDS-PAGE gel for separation. Next, after transferring proteins to membranes, they were blocked with skim milk and were immersed in the primary antibodies at 4°C for one night, including anti-HIF-1α (1:2000) and anti-β-tubulin (1:2000) antibodies.

Finally, after the membranes were immersed in HRP-labeled goat anti-rabbit antibody (1:2000) and stained with ECL chemiluminescent substrate, the grayscale value of each blot was quantified by ImageJ software.

Statistical analysis

Data presented as mean ± SD originated from at least three biological replicates and three independent experiments, and were analyzed using one-way ANOVA followed by Tukey's *post-hoc* test with the help of GraphPad Prism 8.0.2 (La Jolla, CA, USA). In addition, the Bonferroni correction, Shapiro-Wilk test, and Levene's test were used for the adjustment of multiple comparisons and the assessment of the normality and homogeneity of variance, respectively. A p-value <0.05 means statistically significant.

Results

Identification of c-kit+ cells

After the purification, the biomarkers of c-kit$^+$ cells were identified. In the purified c-kit$^+$ cells, the positive rates of c-kit, Scal-1, and CD34, as well as CD45, were 100% and 0%, respectively (Figure 1). The above results demonstrated that we obtained high-purity c-kit$^+$ cells, which were used for the subsequent studies.

Effects of overexpressing miR-199a-5p on c-kit$^+$ cells

The miR-199a-5p expression level in the NC mimics group was similar to the control group, and in the miR-199a-5p mimics group was dramatically higher than the NC mimics group, suggest-

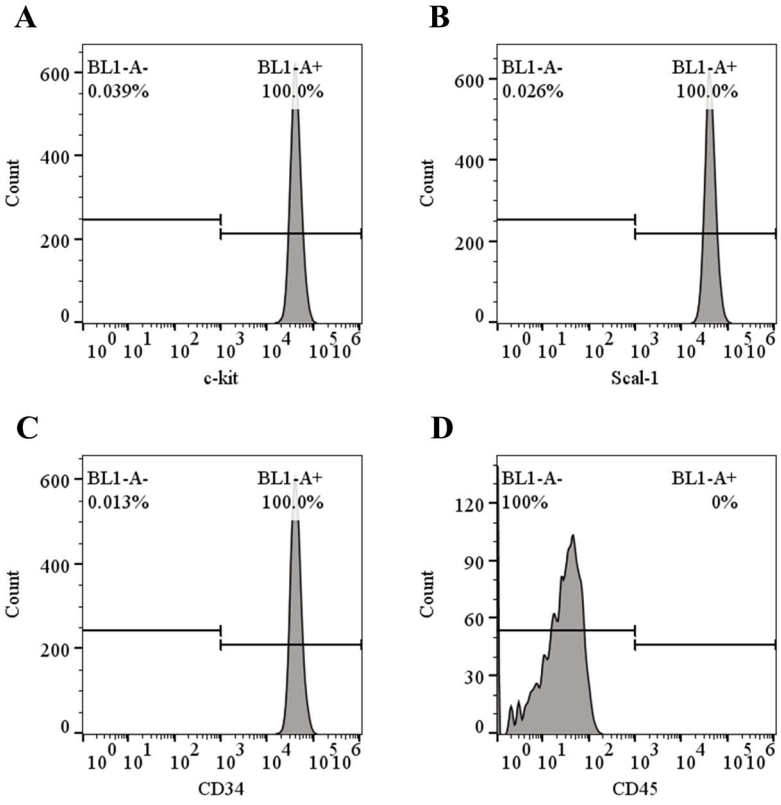

Figure 1. Identification of c-kit$^+$ cells. The three biomarkers of c-kit$^+$ cells, including c-kit (**A**), Scal-1 (**B**), CD34 (**C**), and CD45 (**D**), were identified using the flow cytometry. Data were obtained from three independent experiments.

Table 1. RT-qPCR primer sequences.

Gene	Forward	Reverse
miR-199a-5p	GCGCTTGTCCATCAGACTTG	AGTGCAGGGTCCGAGGTATT
Nkx2.5	CTTCGTGAACTTTGGCGTCG	CGCCCTTCTCCTAAAGGTGG
CD31	AGCCTAGTGTGGAAGCCAAC	AAGGGAGCCTTCCGTTCTCT
α-SMA	GTACCACCATGTACCCAGGC	GCTGGAAGGTAGACAGCGAA
HIF-1α	AGTGCTGATCCTGCACTGAA	AGGCTGGGAAAAGTTAGGAGTG
U6	TCTCGTCTGATCTCGGAAGC	AGCCTACAGCACCCGGTAT
GAPDH	CCCTTAAGAGGGATGCTGCC	TACGGCCAAATCCGTTCACA

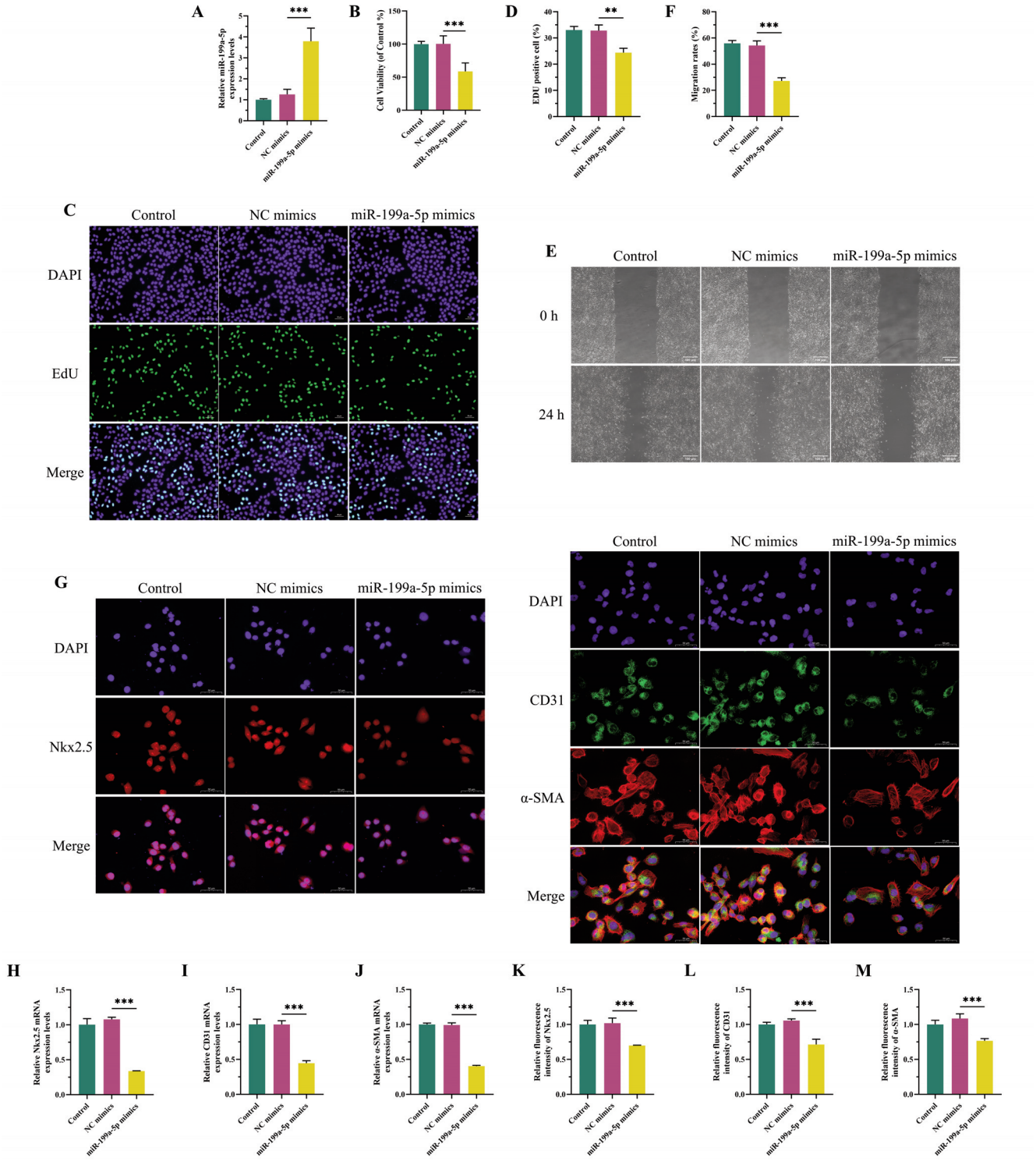

Figure 2. Effects of overexpressing miR-199a-5p on c-kit$^+$ cells. **A**) The miR-199a-5p expression level of c-kit$^+$ cells after overexpressing miR199a-5p was detected by RT-qPCR (n=3). **B**) The cell viability of c-kit$^+$ cells after overexpressing miR199a-5p was detected by the CCK-8 approach (n=6). **C**) The EdU staining results of c-kit$^+$ cells after overexpressing miR199a-5p; scale bar: 50 μm. **D**) The EdU positively stained rate of c-kit$^+$ cells after overexpressing miR199a-5p (n=3). **E**) The wound healing of c-kit$^+$ cells after overexpressing miR199a-5p; scale bar: 100 μm. **F**) The migration rate of c-kit$^+$ cells after overexpressing miR199a-5p (n=3). G) The IF staining results of Nkx2.5, CD31, and α-SMA of c-kit$^+$ cells after overexpressing miR199a-5p; scale bar: 50 μm. The fluorescence intensity of Nkx2.5 (**H**), CD31 (**I**), and α-SMA (**J**) of c-kit$^+$ cells after overexpressing miR199a-5p (n=3). The mRNA expression levels of Nkx2.5 (K), CD31 (**L**), and α-SMA (M) of c-kit$^+$ cells after overexpressing miR199a-5p were detected by RT-qPCR (n=3). Data were obtained from three independent experiments and were analyzed using one-way ANOVA followed by Tukey's *post-hoc* test. ***p<0.001 and **p<0.01 *vs* the NC mimics group.

ing that NC mimics and miR-199a-5p mimics were successfully transfected ($p<0.001$, Figure 2A). The CCK-8 approach, EdU staining, wound healing, RT-qPCR, and IF approaches were subsequently used to determine the effects of overexpressing miR-199a-5p on c-kit$^+$ cells. The cell viability ($p<0.001$), the EdU positively stained cell number ($p<0.01$), the migrated cell ($p<0.001$), and Nkx2.5 ($p<0.001$), CD31 ($p<0.001$), and α-SMA ($p<0.001$) expression of c-kit$^+$ cells in the miR-199a-5p group were prominently lower than the NC mimics group, demonstrating overexpressing miR-199a-5p inhibited the cell viability, proliferation, migration, and differentiation of c-kit$^+$ cells (Figures 2 B-M).

Effects of knocking down HIF-1α on c-kit$^+$ cells

The HIF-1α expression was detected to determine whether si-NC and si-HIF-1α were successfully transfected. The HIF-1α expression was significantly upregulated after establishing the hypoxic model ($p<0.001$). Meanwhile, the HIF-1α expression level in the si-NC group was similar to the model group, and in the si-HIF-1α group was prominently lower than the si-NC group ($p<0.01$), indicating that si-NC and si-HIF-1α were successfully transfected (Figures 3 A-C). The CCK-8 approach, EdU staining, wound healing, RT-qPCR, and IF approaches were subsequently used to determine the effects of knocking down HIF-1α on c-kit$^+$ cells. After establishing the hypoxic model, the cell viability ($p<0.001$), EdU positively stained cell number ($p<0.01$), the migrated cell ($p<0.001$), and Nkx2.5 ($p<0.001$), CD31 ($p<0.001$), and α-SMA ($p<0.001$) expression were substantially downregulated (Figures 3 D-O). In addition, knocking down HIF-1α further reduced the above indicators ($p<0.05$), confirming that knocking down HIF-1α inhibited the cell viability, proliferation, migration, and differentiation of c-kit$^+$ cells.

MiR-199a-5p targeted and suppressed HIF-1α

As the above results affirmed that overexpressing miR-199a-5p and knocking down HIF-1α suppressed the cell viability, proliferation, migration, and differentiation of c-kit$^+$ cells, we subsequently explored whether there was a targeted relationship between miR-199a-5p and HIF-1α. It was attested that overexpressing miR-199a-5p reduced HIF-1α expression ($p<0.01$, Figures 4 A-C). After that, the targeted relation between miR-199a-5p and HIF-1α was determined through the dual-luciferase report experiment. As presented in Figure 4D, there were potential binding sites between HIF-1α and miR-199a-5p. In addition, miR-199a-5p mimics could not alter the relative luciferase unit (RFU) of HIF-1α-MUT but downregulated the RFU of HIF-1α-WT ($p<0.01$, Figure 4E). Moreover, the miR-199a-5p expression level was prominently downregulated ($p<0.001$), and the HIF-1α expression level was dramatically upregulated ($p<0.001$) under the hypoxic condition. Overexpressing miR-199a-5p prominently reduced the HIF-1α expression level under the hypoxic condition as well ($p<0.01$, Figures 4 F-I). The above results affirmed that miR-199a-5p targeted and suppressed HIF-1α.

Overexpressing HIF-1α reversed the effects of overexpressing miR-199a-5p on c-kit$^+$ cells

As we have already affirmed the targeted relation between miR-199a-5p and HIF-1α, we subsequently explored the effects of overexpressing HIF-1α on miR-199a-5p-upregulated c-kit$^+$ cells. The hypoxic model significantly decreased the cell viability ($p<0.001$), EdU positively stained cell number ($p<0.001$), the migrated cell ($p<0.01$), and Nkx2.5 ($p<0.001$), CD31 ($p<0.001$), and α-SMA ($p<0.001$) expression of c-kit$^+$ cells. Overexpressing miR-199a-5p further reduced the above indicators ($p<0.01$). Compared with the miR-199a-5p mimics + oe-NC group, the levels of the above indicators were significantly upregulated in the miR-199a-5p mimics + oe-HIF-1α group ($p<0.05$), proving that overexpressing HIF-1α reversed the effects of up-regulated miR-33a-5p on c-kit$^+$ cells (Figure 5 A-L).

Discussion

In recent years, stem cells have been considered a promising means of heart repair. Previous studies demonstrated that c-kit$^+$ cells, one kind of CSCs, were involved in tumorigenesis, angiogenesis, and maintenance of progenitor cells, and their proliferation, migration, and differentiation were essential to the regeneration of cardiomyocytes.[22,23] Therefore, this study aims to explore the relationship between miR-199a-5p and HIF-1α and their effects on c-kit$^+$ cells, finding safe and effective treatment strategies to protect patients from the harm of MI.

miR-199a-5p, a member of the microRNA family enriched in the myocardium, binds with specific genes that are involved in cardiomyocyte regeneration, cell apoptosis, neovascularization, and cardiac remodeling.[24-26] The previous study reported that miR-199a-5p was elevated in atrial fibrillation and sinus arrhythmia patients based on a circulating miRNA profile analysis of patients with reduced ejection fraction.[27] It was also found that miR-199a-5p was upregulated in cardiomyocytes of mice after MI.[18] However, our study demonstrated that miR-199a-5p was downregulated in c-kit$^+$ cells. We speculated that the differences in miR-199a-5p expression level between the previous study and our study might be derived from the different cell types. In addition, although the previous studies suggested that miR-199a-5p promoted the proliferation and migration of cardiomyocytes, some studies indicated that miR-199a-5p inhibited the proliferation, migration, and differentiation of diverse stem cells.[28-30] In our study, we discovered that overexpressing miR-199a-5p suppressed the proliferation, migration, and differentiation of c-kit$^+$ cells, which were consistent with the previous studies. Moreover, after the binding sites between miR-199a-5p and HIF-1α were predicted by the Target Scan website, the dual-luciferase report, RT-qPCR, and Western blot approaches affirmed that HIF-1α was downstream of miR-199a-5p. Therefore, we speculate that the effects of miR-199-5p on c-kit$^+$ cells were related to targeting and regulating HIF-1α.

HIF-1α, a key regulatory factor, is involved in the development of MI by regulating the biological behavior of diverse cells under hypoxic conditions.[31] In one previous study, we found that myocardial cell apoptosis was inhibited and vascular regeneration and heart function in the infarcted area were improved after transplanting HIF-1α modified CSCs into rats with heart failure after MI.[32] Another study also suggested that HIF-1α enhanced stem cell proliferation, survival, migration, and invasion under hypoxic environments by modulating gene expression related to apoptosis and necrosis.[33] In addition, one previous study also indicated that the upregulation of HIF-1α expression enhanced the differentiation of stem cells.[34] In this study, we found that knocking down HIF-1α suppressed the proliferation, migration, and differentiation of c-kit$^+$ cells, and overexpressing HIF-1α effectively reversed the inhibitory effects of overexpressing miR-199a-5p on c-kit$^+$ cells, which were consistent with the previous studies. In addition, our studies affirmed that the Nkx2.5 and CD31 expression levels in c-kit$^+$ cells were downregulated after establishing the hypoxic model, suggesting that the cardiac regeneration ability was inhibited, and the ability of angiogenesis was reduced, which is consistent with the clinical characteristics of MI.

So far, although we have confirmed that miR-199a-5p negatively targets HIF-1α to inhibit the proliferation, migration, and differentiation of c-kit$^+$ cells in the present study, there are still some limitations. First, it is not entirely sufficient to attest the rela-

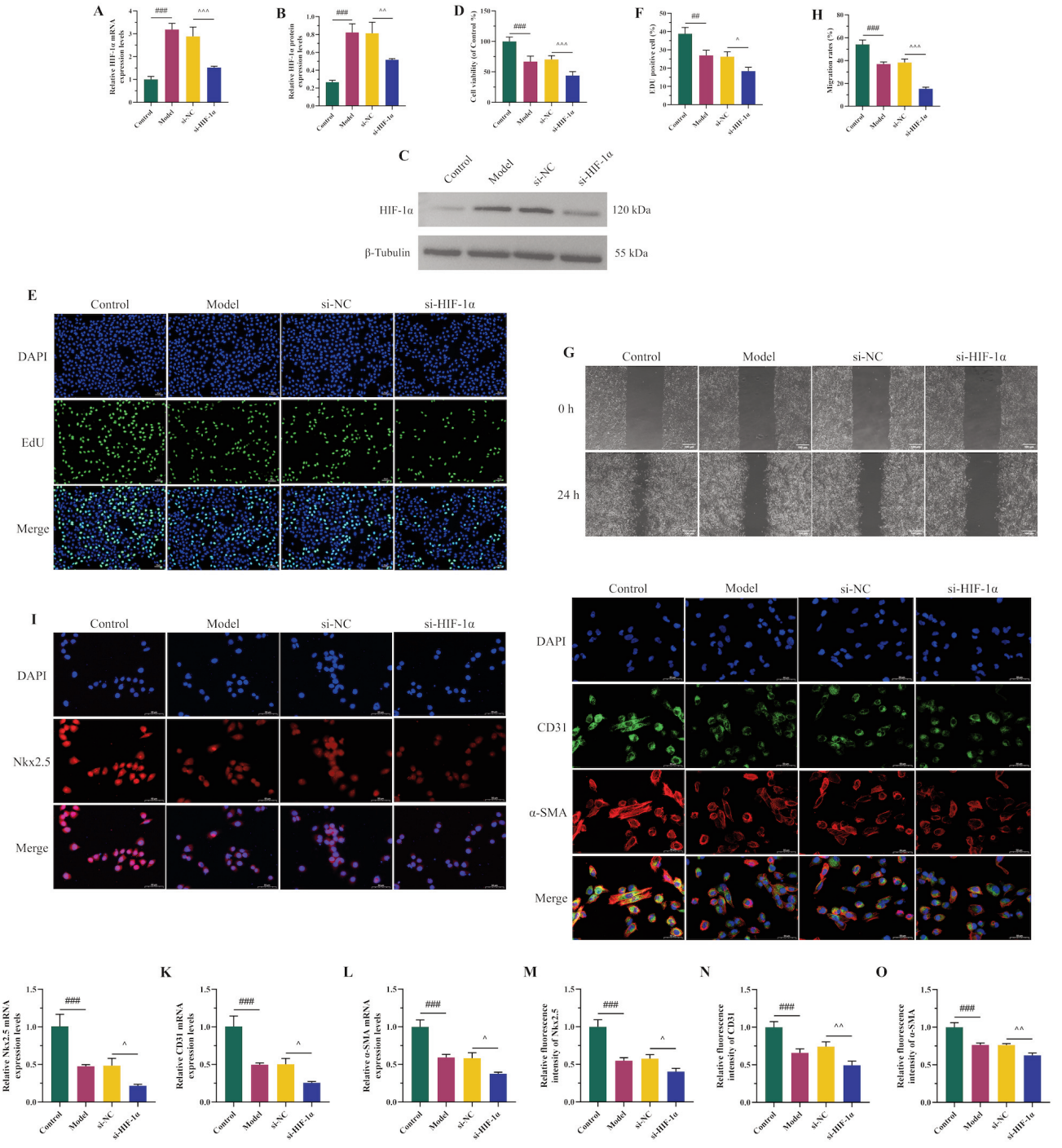

Figure 3. Effects of knocking down HIF-1α on c-kit$^+$ cells. The mRNA (**A**) and protein (**B**) expression levels of HIF-1α in c-kit$^+$ cells after knocking down HIF-1α were detected by RT-qPCR and Western blot approaches (n=3). **C**) The protein blots of HIF-1α and β-Tubulin of c-kit$^+$ cells after knocking down HIF-1α. **D**) The cell viability of c-kit$^+$ cells after knocking down HIF-1α was detected by the CCK-8 approach (n=6). **E**) The EdU staining results of c-kit$^+$ cells after knocking down HIF-1α, scale bar: 50 μm). **F**) The EdU positively stained rate of c-kit$^+$ cells after knocking down HIF-1α (n=3). **G**) The wound healing of c-kit$^+$ cells after knocking down HIF-1α; scale bar: 100 μm). H) The migration rate of c-kit$^+$ cells after knocking down HIF-1α (n=3). **I**) The immunofluorescence staining results of Nkx2.5, CD31, and α-SMA of c-kit$^+$ cells after knocking down HIF-1α; scale bar: 50 μm. The fluorescence intensity of Nkx2.5 (**J**), CD31 (K), and α-SMA (**L**) of c-kit$^+$ cells after knocking down HIF-1α (n=3). The mRNA expression levels of Nkx2.5 (**M**), CD31 (**N**), and α-SMA (**O**) of c-kit$^+$ cells after knocking down HIF-1α were determined by RT-qPCR (n=3). Data were obtained from three independent experiments and were analyzed using one-way ANOVA followed by Tukey's *post-hoc* test. $^{###}p<0.001$ and $^{##}p<0.01$ *vs* the control group; $^{\wedge\wedge\wedge}p<0.001$, $^{\wedge\wedge}p<0.05$ and $^{\wedge}p<0.05$ *vs* the si-NC group.

tion between miR-199a-5p and HIF-1α and their effects on c-kit$^+$ cells. It is more important to validate our findings *in vivo* further. Therefore, it is necessary to conduct related animal experiments to further evidence our findings in the subsequent studies. For instance, after administering miR-199a-5p activator or inhibitor to mice, determining the cardiac functions and myocardial injuries, as well as the miR-199a-5p and HIF-1α expression in CSCs isolated by flow cytometry, would be conducive to further confirming our conclusion. Besides, apart from the c-kit$^+$ cells, there are some other CSC lineages, such as Sca-1$^+$ and Islet-1$^+$ cells.[35] miR-199a-5p and HIF-1α may also generate regulated effects on the proliferation, migration, and differentiation of another kind of CSC lineage. It was demonstrated that the Sca-1$^+$ cells were highly expressed in arterial endothelial cells after atherosclerosis, which

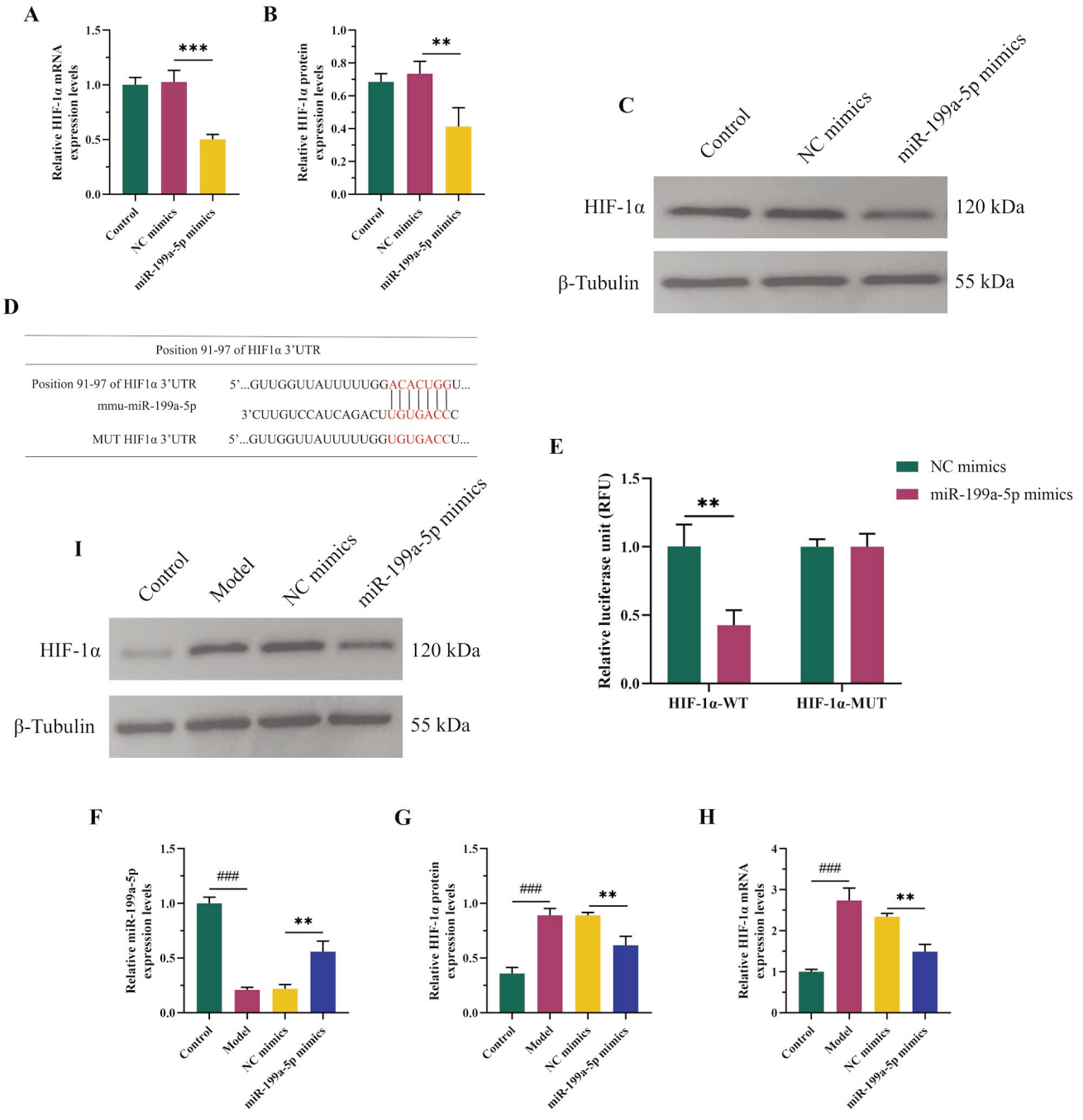

Figure 4. miR-199a-5p targeted and suppressed HIF-1α. The mRNA (**A**) and protein (**B**) expression levels of HIF-1α in c-kit$^+$ cells (n=3). **C**) The protein blots of HIF-1α and β-Tubulin of c-kit$^+$ cells. **D**) The predicted binding sites between miR-119a-5p and HIF-1α. **E**) The results of the dual-luciferase report experiment between miR-119a-5p and HIF-1α (n=3). **F**) The miR-119a-5p expression level in hypoxic c-kit$^+$ cells (n=3). The mRNA (**G**) and protein (**H**) expression levels of HIF-1α in hypoxic c-kit$^+$ cells (n=3). **I**) The protein blots of HIF-1α and β-Tubulin of hypoxic c-kit$^+$ cells. Data were obtained from three independent experiments and were analyzed using one-way ANOVA followed by Tukey's *post-hoc* test. $^{###}p<0.001$ *vs* the control group, $^{***}p<0.001$ and $^{**}p<0.01$ *vs* the NC mimics group.

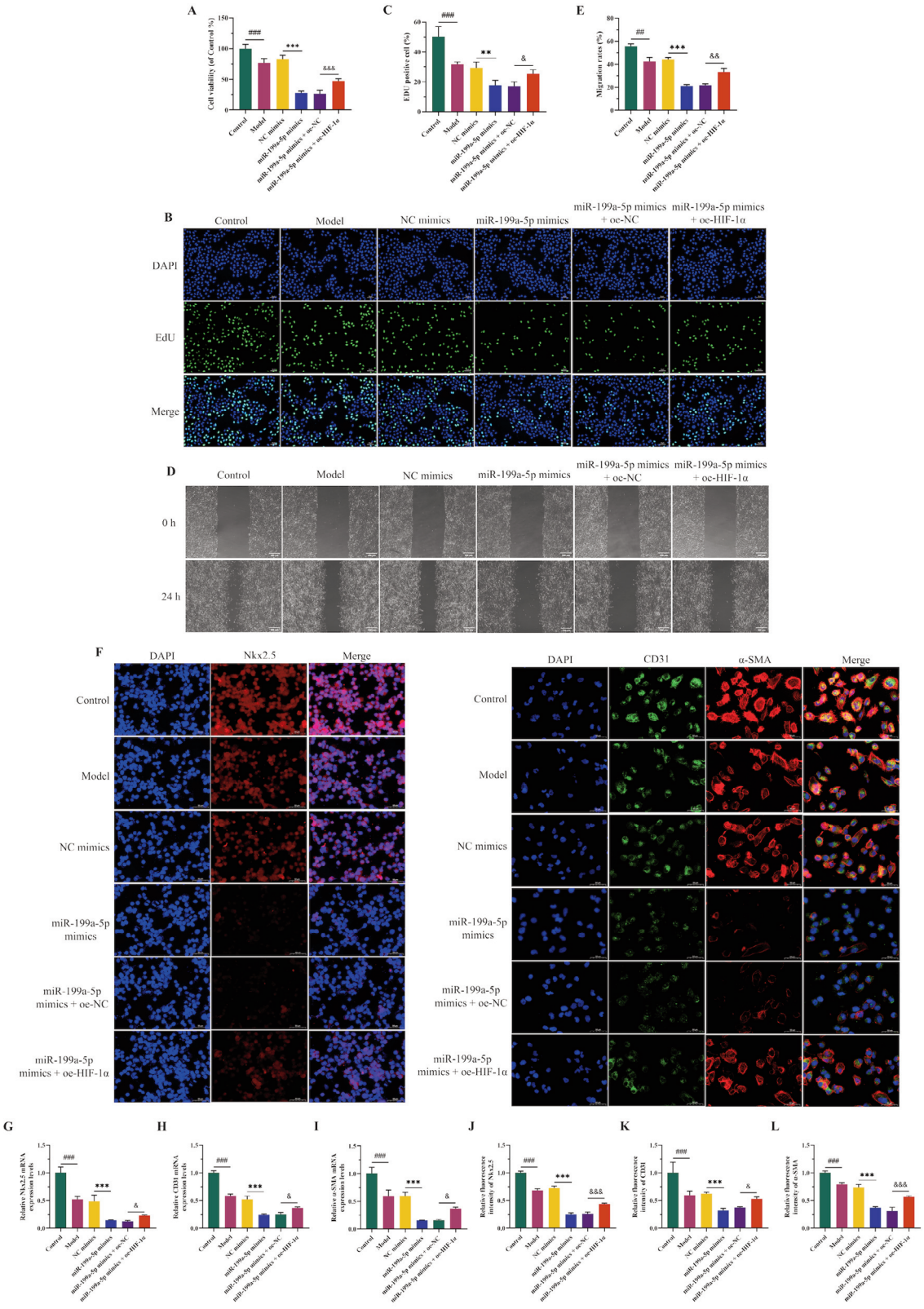

Figure 5. Overexpressing HIF-1α reversed the effects of overexpressing miR-199a-5p on c-kit$^+$ cells. **A**) The cell viability of c-kit$^+$ cells was detected by the CCK-8 approach (n=6). **B)** The EdU staining results of c-kit$^+$ cells; scale bar: 50 μm. **C**) The EdU positively stained rate of c-kit$^+$ cells (n=3). **D**) The wound healing of c-kit$^+$ cells; scale bar: 100 μm. **E**) The migration rate of c-kit$^+$ cells (n=3). **F**) The immunofluorescence staining results of Nkx2.5, CD31, and α-SMA of c-kit$^+$ cells; scale bar: 50 μm. The fluorescence intensity of Nkx2.5 (**G**), CD31 (**H**), and α-SMA (**I**) of c-kit$^+$ cells (n=3). The mRNA expression level of Nkx2.5 (J), CD31 (K), and α-SMA (L) of c-kit$^+$ cells was detected by RT-qPCR (n=3). Data were obtained from three independent experiments and were analyzed using one-way ANOVA followed by Tukey's *post-hoc* test. $^{###}p<0.001$ and $^{##}p<0.01$ *vs* the control group; $^{***}p<0.001$ and $^{**}p<0.01$ *vs* the NC mimics group; $^{\&\&\&}p<0.001$, $^{\&\&}p<0.01$ and $^{\&}p<0.05$ *vs* the miR-199a-5p mimics $^+$ oe-NC group.

played an important role in the repair of vascular endothelium.[36] In addition, Islet-1$^+$ CSCs were reported to differentiate into cardiomyocytes to promote myocardial tissue repair after MI.[37] Therefore, we believe that further investigations on the effects of miR-199a-5p and HIF-1α on another kind of CSC lineage, such as Islet-1$^+$ CSCs, could also be beneficial for the clinical treatment of MI. Moreover, we consider that the lack of exploration of downstream mechanisms of HIF-1α is another shortcoming of the present study. A previous study demonstrated that HIF-1α not only participates in the development and reconstruction of blood vessels through regulating downstream VEGF, PDGF, and FGF, but also is involved in the regulation of vascular tension by mediating nitric oxide synthase, adrenergic receptors, and glycolysis.[38] Therefore, we believe that exploring the downstream mechanisms of HIF-1α contributes to improving the clinical treatment strategies of MI.

Taken together, this study demonstrated that miR-199a-5p negatively targeted HIF-1α to inhibit the proliferation, migration, and differentiation of c-kit$^+$ cells, providing a novel strategy for the clinical treatment of MI.

References

1. Frantz S, Hundertmark MJ, Schulz-Menger J, Bengel FM, Bauersachs J. Left ventricular remodelling post-myocardial infarction: pathophysiology, imaging, and novel therapies. Eur Heart J 2022;43:2549-61.
2. Wilcox JE, Fang JC, Margulies KB, Mann DL. Heart failure with recovered left ventricular ejection fraction: JACC scientific expert panel. J Am Coll Cardiol 2020;76:719-34.
3. Guglin M, Zucker MJ, Borlaug BA, Breen E, Cleveland J, Johnson MR, et al. Evaluation for heart transplantation and LVAD implantation: JACC council perspectives. J Am Coll Cardiol 2020;75:1471-87.
4. Hou J, Wang L, Jiang J, Zhou C, Guo T, Zheng S, et al. Cardiac stem cells and their roles in myocardial infarction. Stem Cell Rev Rep 2013;9:326-38.
5. Mancuso A, Barone A, Cristiano MC, Cianflone E, Fresta M, Paolino D. Cardiac stem cell-loaded delivery systems: a new challenge for myocardial tissue regeneration. Int J Mol Sci 2020;21:7701.
6. Matsa E, Sallam K, Wu JC. Cardiac stem cell biology: glimpse of the past, present, and future. Circ Res 2014;114:21-7.
7. Wang K, Ding R, Ha Y, Jia Y, Liao X, Wang S, et al. Hypoxia-stressed cardiomyocytes promote early cardiac differentiation of cardiac stem cells through HIF-1alpha/Jagged1/Notch1 signaling. Acta Pharm Sin B 2018;8:795-804.
8. Hnatiuk AP, Ong SG, Olea FD, Locatelli P, Riegler J, Lee WH, et al. Allogeneic mesenchymal stromal cells overexpressing mutant human hypoxia-inducible factor 1-alpha (HIF1-alpha) in an ovine model of acute myocardial infarction. J Am Heart Assoc 2016;5:e003714.
9. Cheng Y, Feng Y, Xia Z, Li X, Rong J. ω-Alkynyl arachidonic acid promotes anti-inflammatory macrophage M2 polarization against acute myocardial infarction via regulating the cross-talk between PKM2, HIF-1alpha and iNOS. Biochim Biophys Acta Mol Cell Biol Lipids 2017;1862:1595-605.
10. Gabisonia K, Prosdocimo G, Aquaro GD, Carlucci L, Zentilin L, Secco I, et al. MicroRNA therapy stimulates uncontrolled cardiac repair after myocardial infarction in pigs. Nature 2019;569:418-22.
11. Chen Y, Li S, Zhang Y, Wang M, Li X, Liu S, et al. The lncRNA Malat1 regulates microvascular function after myocardial infarction in mice via miR-26b-5p/Mfn1 axis-mediated mitochondrial dynamics. Redox Biol 2021;41:101910.
12. Zheng H, Huang S, Wei G, Sun Y, Li C, Si X, et al. CircRNA Samd4 induces cardiac repair after myocardial infarction by blocking mitochondria-derived ROS output. Mol Ther 2022;30:3477-98.
13. Li B, Meng X, Zhang L. microRNAs and cardiac stem cells in heart development and disease. Drug Discov Today 2019;24:233-40.
14. Huang H, Xie S, Gu X, Xiang B, Zhong Z, Huang P, et al. Higher circulating miR-199a-5p indicates poor aerobic exercise capacity and associates with cardiovascular dysfunction during chronic exposure to high altitude. Front Physiol 2021;12:587241.
15. Hu J, Huang X, Zheng L, Zhang Y, Zeng H, Nie L, et al. MiR-199a-5P promotes osteogenic differentiation of human stem cells from apical papilla via targeting IFIT2 in apical periodontitis. Front Immunol 2023;14:1149339.
16. Geng Y, Hua H, Xia Y, Zhou J, He J, Xu X, et al. miR-199a-5p modulates choroidal neovascularization by regulating Wnt7b/Wnt/β-catenin signaling pathway. J Mol Histol 2024;55:359-70.
17. Chen Y, Liu S, Liang Y, He Y, Li Q, Zhan J, et al. Single dose of intravenous miR199a-5p delivery targeting ischemic heart for long-term repair of myocardial infarction. Nat Commun 2024;15:5565.
18. Asensio-Lopez MC, Sassi Y, Soler F, Fernandez DPM, Pascual-Figal D, Lax A. The miRNA199a/SIRT1/P300/Yy1/sST2 signaling axis regulates adverse cardiac remodeling following MI. Sci Rep-Uk 2021;11:3915.
19. Lampert MA, Orogo AM, Najor RH, Hammerling BC, Leon LJ, Wang BJ, et al. BNIP3L/NIX and FUNDC1-mediated mitophagy is required for mitochondrial network remodeling during cardiac progenitor cell differentiation. Autophagy 2019;15:1182-98.
20. Li J, Song F, Chen R, Yang J, Liu J, Huang L, et al. Bradykinin-pretreated human cardiac-specific c-kit(+) cells enhance exosomal miR-3059-5p and promote angiogenesis against hindlimb ischemia in mice. Stem Cell Rev Rep 2023;19:2481-96.
21. Feng J, Zhan J, Ma S. LRG1 promotes hypoxia-induced cardiomyocyte apoptosis and autophagy by regulating hypoxia-inducible factor-1alpha. Bioengineered 2021;12:8897-907.
22. Cimini M, Fazel S, Zhuo S, Xaymardan M, Fujii H, Weisel RD, et al. c-kit dysfunction impairs myocardial healing after infarction. Circulation 2007;116:I77-82.
23. Gude NA, Sussman MA. Chasing c-Kit through the heart: Taking a broader view. Pharmacol Res 2018;127:110-5.
24. Zeng N, Huang YQ, Yan YM, Hu ZQ, Zhang Z, Feng JX, et al. Diverging targets mediate the pathological role of miR-199a-5p and miR-199a-3p by promoting cardiac hypertrophy and fibrosis. Mol Ther Nucl Acids 2021;26:1035-50.
25. Phatak P, Tulapurkar ME, Burrows WM, Donahue JM. MiR-199a-5p decreases esophageal cancer cell proliferation partially through repression of Jun-B. Cancers 2023;15:4811.
26. Xu M, Zhang J, Lu X, Liu F, Shi S, Deng X. MiR-199a-5p-regulated SMARCA4 promotes oral squamous cell carcinoma tumorigenesis. Int J Mol Sci 2023;24:4756.
27. Garcia-Elias A, Tajes M, Yanez-Bisbe L, Enjuanes C, Comin-Colet J, Serra SA, et al. Atrial fibrillation in heart failure is associated with high levels of circulating microRNA-199a-5p and 22-5p and a defective regulation of intracellular calcium and cell-to-cell communication. Int J Mol Sci 2021;22:10377.
28. Chen HY, Lu J, Wang ZK, Yang J, Ling X, Zhu P, et al. Hsa-miR-199a-5p protect cell injury in hypoxia induces myocardial

cells via targeting HIF1alpha. Mol Biotechnol 2022;64:482-92.
29. Mobus S, Yang D, Yuan Q, Ludtke TH, Balakrishnan A, Sgodda M, et al. MicroRNA-199a-5p inhibition enhances the liver repopulation ability of human embryonic stem cell-derived hepatic cells. J Hepatol 2015;62:101-10.
30. Lu RH, Xiao ZQ, Zhou JD, Yin CQ, Chen ZZ, Tang FJ, et al. MiR-199a-5p represses the stemness of cutaneous squamous cell carcinoma stem cells by targeting Sirt1 and CD44ICD cleavage signaling. Cell Cycle 2020;19:1-14.
31. Pan J, Zhang L, Li D, Li Y, Lu M, Hu Y, et al. Hypoxia-inducible factor-1: Regulatory mechanisms and drug therapy in myocardial infarction. Eur J Pharmacol 2024;963:176277.
32. Li S, Li S. Effects of transplantation of hypoxia-inducible factor-1alpha gene-modified cardiac stem cells on cardiac function of heart failure rats after myocardial infarction. Anatol J Cardiol 2018;20:318-29.
33. Kakudo N, Morimoto N, Ogawa T, Taketani S, Kusumoto K. Hypoxia enhances proliferation of human adipose-derived stem cells via HIF-1a activation. Plos One 2015;10:e0139890.
34. Boso D, Rampazzo E, Zanon C, Bresolin S, Maule F, Porcu E, et al. HIF-1alpha/Wnt signaling-dependent control of gene transcription regulates neuronal differentiation of glioblastoma stem cells. Theranostics 2019;9:4860-77.
35. Bollini S, Smart N, Riley PR. Resident cardiac progenitor cells: at the heart of regeneration. J Mol Cell Cardiol 2011;50:296-303.
36. Toledo-Flores D, Williamson A, Schwarz N, Fernando S, Dimasi C, Witt TA, et al. Vasculogenic properties of adventitial Sca-1(+)CD45(+) progenitor cells in mice: a potential source of vasa vasorum in atherosclerosis. Sci Rep 2019;9:7286.
37. Camberos V, Baio J, Mandujano A, Martinez AF, Bailey L, Hasaniya N, et al. The impact of spaceflight and microgravity on the human Islet-1+ cardiovascular progenitor cell transcriptome. Int J Mol Sci 2021;22:3577.
38. Zheng J, Chen P, Zhong J, Cheng Y, Chen H, He Y, et al. HIF-1α in myocardial ischemia-reperfusion injury (Review). Mol Med Rep 2021;23:352.

Received: 21 May 2025. Accepted: 13 August 2025.

European Journal of Histochemistry 2025; 69:4239
doi:10.4081/ejh.2025.4239